Susceptibility Investigation of Debris Flow Hazard Using Topographic Index in the Nakhon Si Thammarat, Southern Thailand

Nutsorn Jaitum and Santi Pailoplee*

Earth Science Program, Department of Geology, Faculty of Science, Chulalongkorn University, Bangkok 10330, Thailand
* Corresponding author email: Pailoplee.S@gmail.com

Received: 21 Feb 2022
Revised: 10 Apr 2022
Accepted: 20 May 2022

Abstract

Nakhon Si Thammarat (NST) is one of the cities in Southern Thailand that is vulnerable to geohazards, such as debris flows, landslides, and flooding, all of which have the potential to cause significant damage to people and property. Several topographic factors could be potential sources of debris flow, including i) a high angle slope of the mountain and ii) a number of mountain-front outlets. Thus, in this study, we used the Frequency Ratio (FR) method to identify and develop the map of debris flow susceptibility area in NST. The topographic indices associated with debris flow activity are analyzed using terrain data obtained from a Digital Elevation Model (DEM) with a resolution of 12.5 meters. The FR was calculated using a combination of ten parameters representing debris flow vulnerable areas, which included: i) slope, ii) aspect, iii) solar radiation, iv) profile curvature, v) plan curvature, vi) topographic wetness index, vii) stream power index, viii) Melton ruggedness number ix) terrain ruggedness index, and x) topographic position index. According to the results, the debris flow susceptibility of NST can be divided into five levels, with high and very high classes found at the Khao Luang Mountain around the center of NST. The eastern and western NST areas were identified as medium and low classes.

Keywords: Nakhon Si Thammarat, Debris Flow, Topographic Index, Mass Wasting, Alluvial Fan

1. Introduction

Mass wasting is a geological term that refers to the downward movement of rocks, soil, mud, and snow along a slope. Geologically, mass wasting can be classified into several categories based on i) type of mass such as rocks, soil, snow, ii) the amount of water, and iii) movement patterns such as drop, collapse, avalanche, slip, and flow. These three factors are the result of different mass migration patterns in terms of speed, size, and the area and level of the potential disaster, such as rock fall, landslide, rockslide, debris avalanche, including debris flow, and so on.

In southern Thailand, NST is the second largest province in the region after Surat Thani, covering 10,170 km^2. Geographically, NST is located between latitude 8˚-9˚19’ north and longitude 99˚15’-100˚15’ east. The following boundaries are adjacent: Surat Thani is to the north; Phatthalung and Songkhla are to the south; the Gulf of Thailand is to the east; and Krabi and Trang are to the west. The regional topography of NST is composed of mountainous areas in the west and the coastal plains in the east.

In the past, NST has been prone to hazards such as debris, landslides, and flash floods. The dangers of these natural disasters can result in significant personal and property damage. For instance, in 1988, flood hazard occurred in the districts of Phipun and Lan Saka. Twenty years later, in 2011, a catastrophe took place in Khanom, Sichon and Nopphitam districts. This resulted in severe damage, such as approximately 230 people were injured and killed, as well as severe damage to agricultural land, livestock, and public services.

To assess the debris-flow hazard areas in NST, we used topographic analysis, remote sensing, and GIS in this study to determine and

zone the potential risk areas of NST. The Frequency Ratio (FR) method is used widely for landslide susceptibility assessment with good performance (Regmi, A.D., 2014). It is a statistical method for simulating environmental conditions that uses factors related to the dependent variable. It was utilized to align all obtained topographic indices in terms of the FR score, which represents the debris-flow susceptibility. The results obtained here could be beneficial in contributing to the debris-flow hazard mitigation plan.

In order to analyze the area sensitive to debris flow (Figure 1), the base data of digital elevation model (DEM) with resolution 12.5 meters are used. After that, 10 topographic index factors were analyzed spatially covering NST, i.e., slope, aspect, solar radiation, curvature plan, and profile curvature. These parameters were analyzed by the ArcGIS software. Meanwhile, the SAGA software was used to calculate the topographic wetness index (TWI), stream power index (SPI), topographic position index (TPI), Melton ruggedness number (MRN), and terrain ruggedness index (TRI). After analyzing all topographic indices for debris flow recognition, the FR approach was used to compute all indices in terms of score. Following that, FR were classified according to their susceptibility to debris flows. According to **Table 1**, FR in this study was classified into five categories: very low, low, medium, high, and very high. Finally, the debris flow susceptibility was mapped according to Meinhardt et al. (2015) method. The maps obtained in this study were validated against the debris flow hazards posed in NST. This record is available in the database of the Department of Mineral Resources as shown in Figure 2.

2. Topographic Index

2.1. Slope

The slope is the most commonly used factor in debris flow. The slope of NST (Figure 3a) ranged from 0° to 70°. The average gradient in most regions was 0°-12°. The maximum value was in Khao Luang area, in the center of NST with 35°-90°.

Before susceptibility calculation, this investigation can divide slope gradient into five classes following to M.Y. Esper Angillieri, 2020: class 1 (0°-12°), class 2 (12°-21°), class 3 (21°-28°), class 4 (28°-35°), and class 5 (35°-90°). Class 1 was primarily found in the eastern and western of NST. Other classes were located at the center of NST, which is a mountain range.

Table 1. Classification of debris flow susceptibility in this study.

Class of debris flow susceptibility	Interval of debris flow susceptibility
Very low	0.85 to 0.38
Low	6.38 to 7.91
Medium	7.91 to 9.17
High	9.17 to 10.80
Very high	10.80 to 14.27

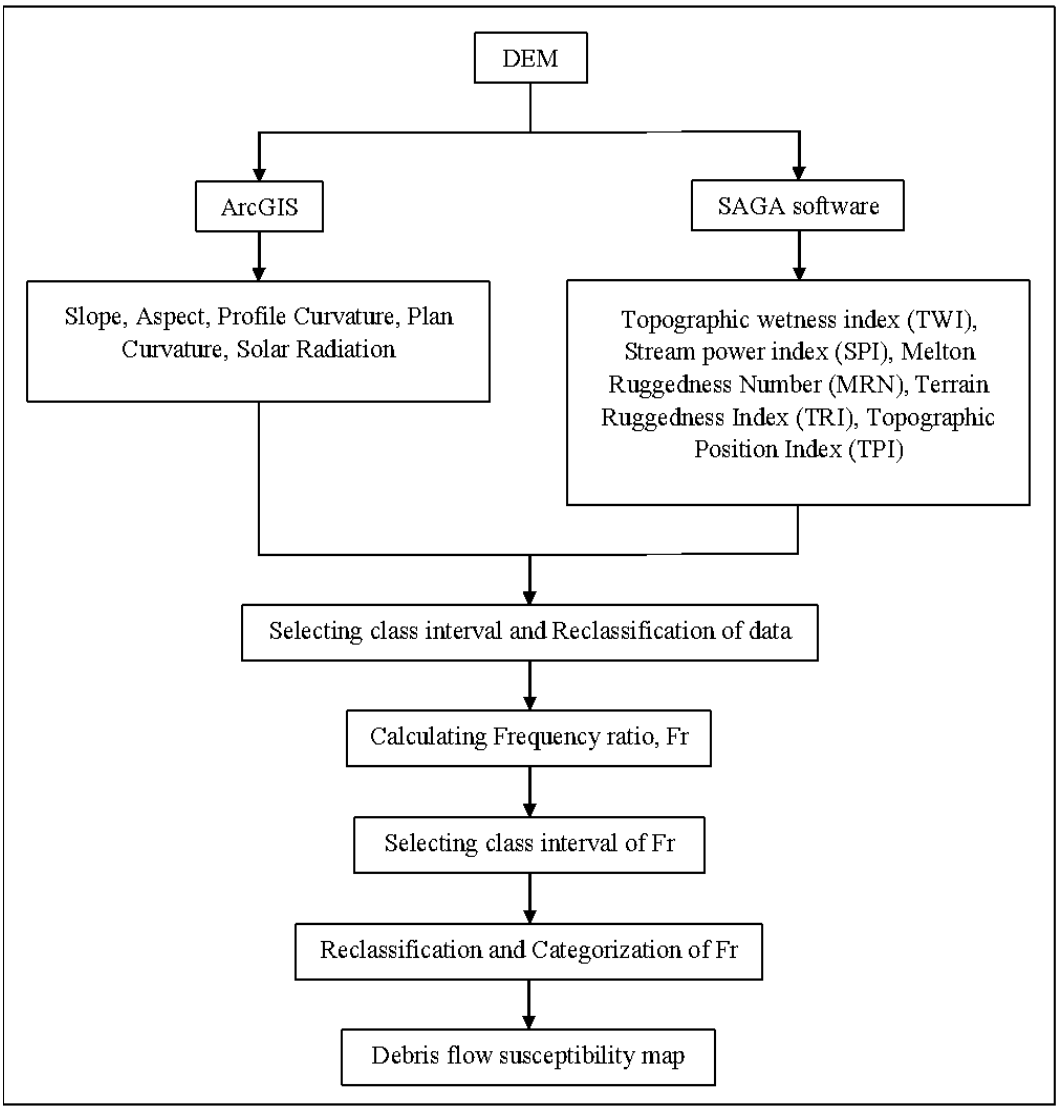

Figure 1. Flowchart showing methodology to analyze debris flow susceptibility in this study

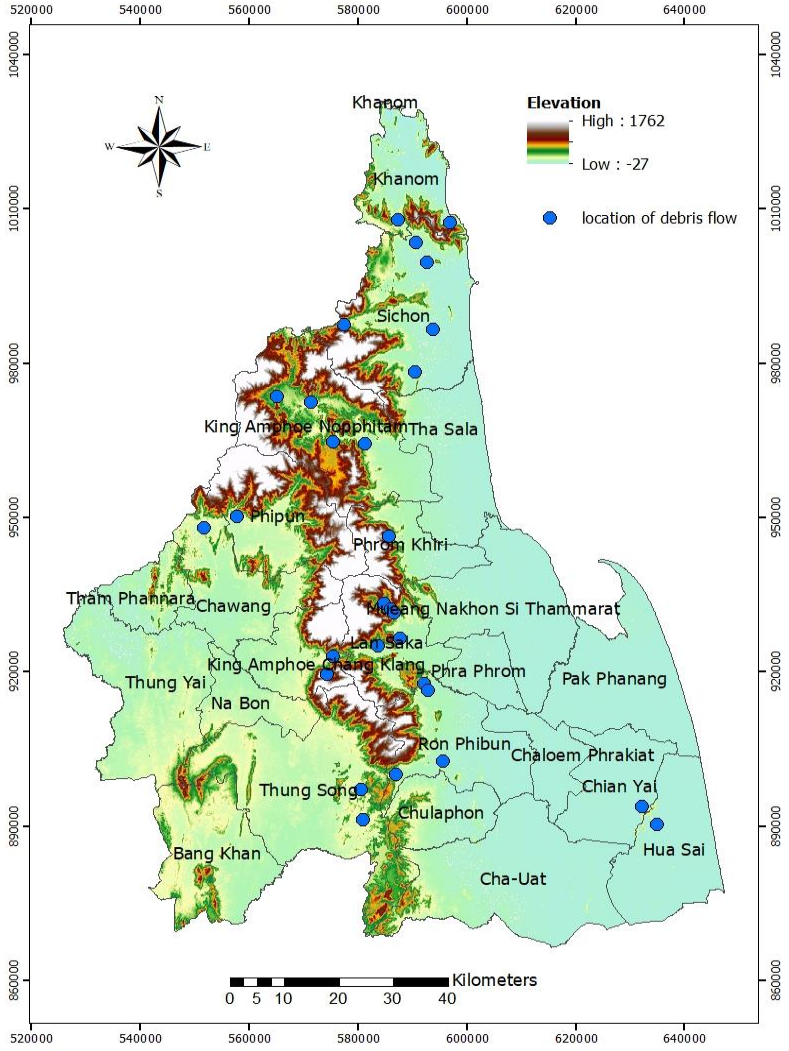

Figure 2. Map of NST showing the location of the debris flow hazard (blue dot) has been posed previously. All data reported and recorded by the Department of Mineral Resource.

2.2. Aspect

The aspect (Figure 3b) can be grouped into four classes and four slope directions, including: i) north, ii) east, iii) south, and iv) west. The evaluation suggests that the majority of the study area represented the flat direction with 2,585 km^2. The second one was the west direction with 2,340 km^2 (Table 2).

2.3. Solar Radiation

Solar radiation in NST (Figure 3c) ranged from 1.78 x^{10-5-} to 9.06 x^{10-5}. The average solar radiation was 5.42 x^{10-5}. The maximum value was 9.06 x^{10-5} , which was located at the mountain range in the center of NST. The majority of solar radiation values in the study area was 7.37 x^{10-5-} to 7.75 x^{10-5} (Table 2).

2.4. Profile Curvature

Profile curvature (Figure 3d) is the vertical curve parallel to the highest direction of the slope. It can be divided into three classes: i) concave, ii) plain and iii) convex zones. They are associated with the flow speed ranging from slow to fast, with positive and negative values, respectively.

According to the analysis, the concave with positive values covers the smallest region in NST, which was equivalent to 0 km^2 scattered around the Khao Luang. The plain covered the majority of NST with 9,724 km^2. Thus, the positive value, which identifies convex, covered 1 km^2 (Table 2).

2.5. Plan Curvature

Plan curvature (Figure 3e) corresponds to the curvature at right angles to the direction of the highest slope. It can be classified into three classes: i) concave, ii) plain, and iii) convex. They may identify an inward-outward flow of the surface after negative to positive values.

According to the results, the negative value, which identifies concave, covered the smallest area of NST, with only 0 km^2. The majority of the NST area was covered by the plain with 9,724 km^2. Additionally, the positive value, which identifies convex, covered 0 km^2 (Table 2).

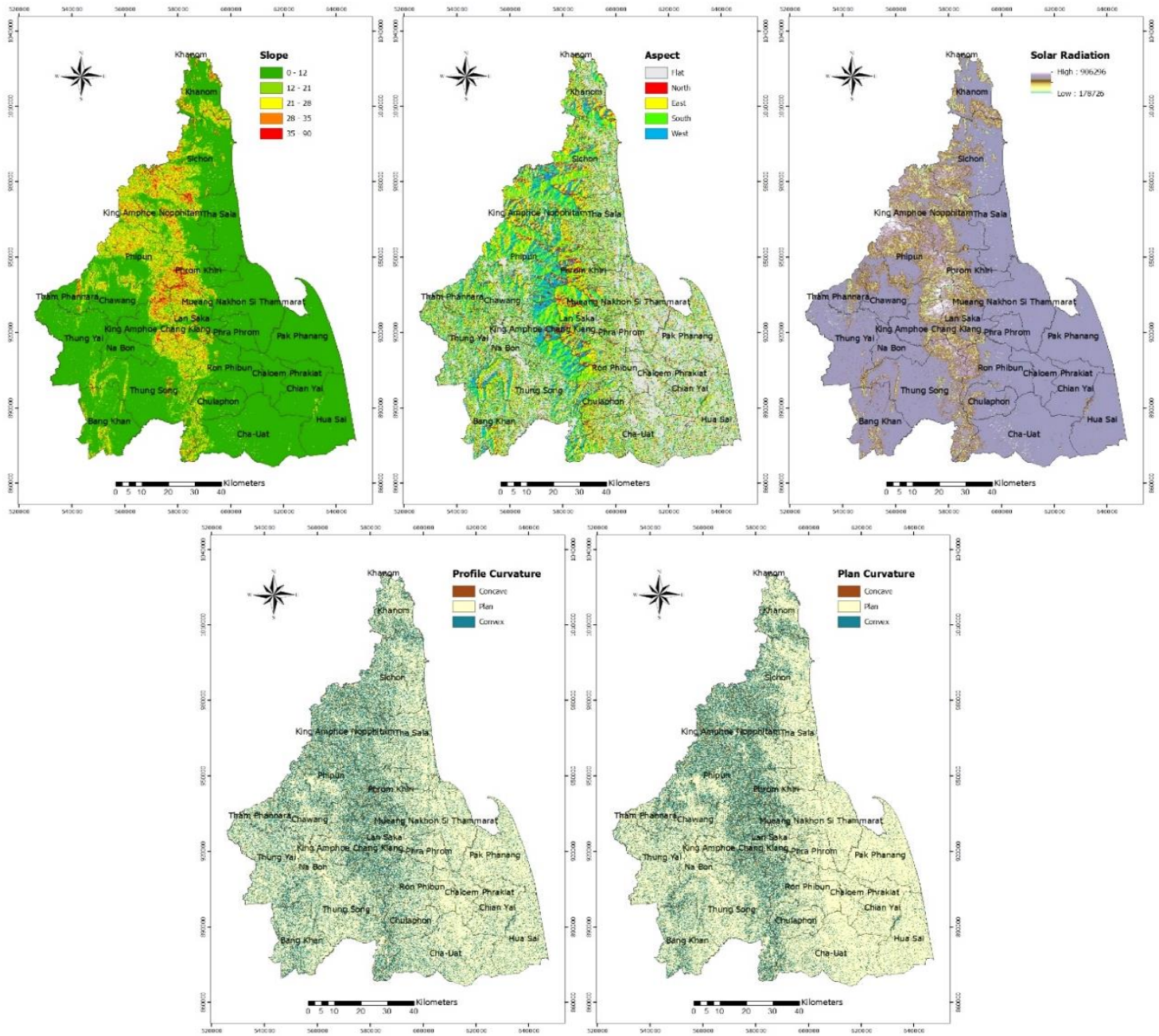

Figure 3. Map of NST showing the topographic index related to the debris flow susceptibility. (a) slope gradient, (b) aspect, (c) solar radiation, (d) profile curvature, (e) plan curvature.

2.6. Topographic Wetness Index

TWI is a measure of soil moisture content that is controlled by topography. It controls the flow direction of soil and groundwater (Rodhe and Seibert, 1999). TWI in NST (Figure 4a) ranged from 0.6 to 26. The majority of the areas had an average TWI of 9 to 12. The maximum value was 26, located at the eastern and western NST. Furthermore, the minimum TWI value (0.6-0.7) was shown in the center area of Khao Luang that defines the mountain peak (Table 2).

Before debris flow susceptibility calculation, TWI can be divided into five classes following Meinhardt et al. (2015): class 1 (0.60-0.70), class 2 (7.00-9.00), class 3 (9.00-12.00), class 4 (12.00-15.00) and class 5 (15.00-26.00). Class 2 was primarily discovered at the center of NST. Whereas, classes 3, 4, and 5 were located at the east and west of NST, which is the plain area. A higher TWI value indicates a higher soil water content and a higher likelihood of debris flow (Chen et al., 2011).

2.7. Stream Power Index

The stream power index (SPI) is used to describe the erosion of flow that may occur at point of terrain surface. SPI in NST (Figure 4b) ranged from -42 to -5,040. The majority of areas have an average SPI of -42 to -43. The minimum SPI was found in the east and west of the NST region. In addition, the maximum SPI was discovered at the center of NST, which indicates a mountain range at 5,040.

Before debris flow susceptibility calculation, SPI can be separated into five classes, including: class 1 -42, class 2 (-42 to 43) class 3 (43 to 187), class 4 (187 to 530) and class 5 (530 to 5,037) (Figure 3g). The majority of the study area was identified as Class 2. The rest classes were located at the center of NST (Figure 3g). A higher SPI value indicates the power of a higher current. (Marchi and Dalla Fontana, 2005) (Table 2).

2.8. Melton Ruggedness Number

The Melton ruggedness number (MNR) is a slope index that provides a specialized representation of the roughness of the terrain within a basin (Melton, 1965). MRN in NST (Figure 4c) ranged from 0 to -29.3939 with an average value of 14.5. The maximum value was 8.00-29.3939, which was found in the mountain range area at the center of NST. The minimum value was 0.00, which was located at the flat area at the west and the east of NST. The high MRN values were found most in the mountains and along the valley area which are consistent with erosion processes and sediment movement (Figure 4c and Table2).

2.9. Terrain Ruggedness Index

Terrain ruggedness index (TRI) (Figure 4d) was grouped into seven classes (Riley et al, 1999): i) level, ii) nearly level, iii) slightly rugged, iv) intermediately rugged, v) moderately rugged, vi) highly rugged, and vii) extremely rugged.

According to the assessment, the majority of the study areas represent level and nearly level with 4,066 and 3,437 km^2, respectively. Aside from that, there are i) slightly rugged (1,159 km^2), ii) intermediately rugged (711 km^2), iii) moderately rugged (292 km^2), iv) highly rugged (53 km^2), and v) extremely rugged (6 km^2). The minimum number of pixels was found in the center of the NST. TRI revealed that the debris formed on highly rugged terrain.

2.10. Topographic Position Index

The topographic position index is negative in concavities such as valley bottoms, positive on crests and peaks and near zero on flat surfaces. TPI of NST (Figure 4e) ranged from -85 to 111. The majority of the study areas had an average TPI of -2 to 111. The maximum value was found in the east and the west of NST. On the other hand, the minimum value was discovered in the center of NST, which points to a mountain range at -85 to -2). TPI found a large amount of debris flow in the valley bottom.

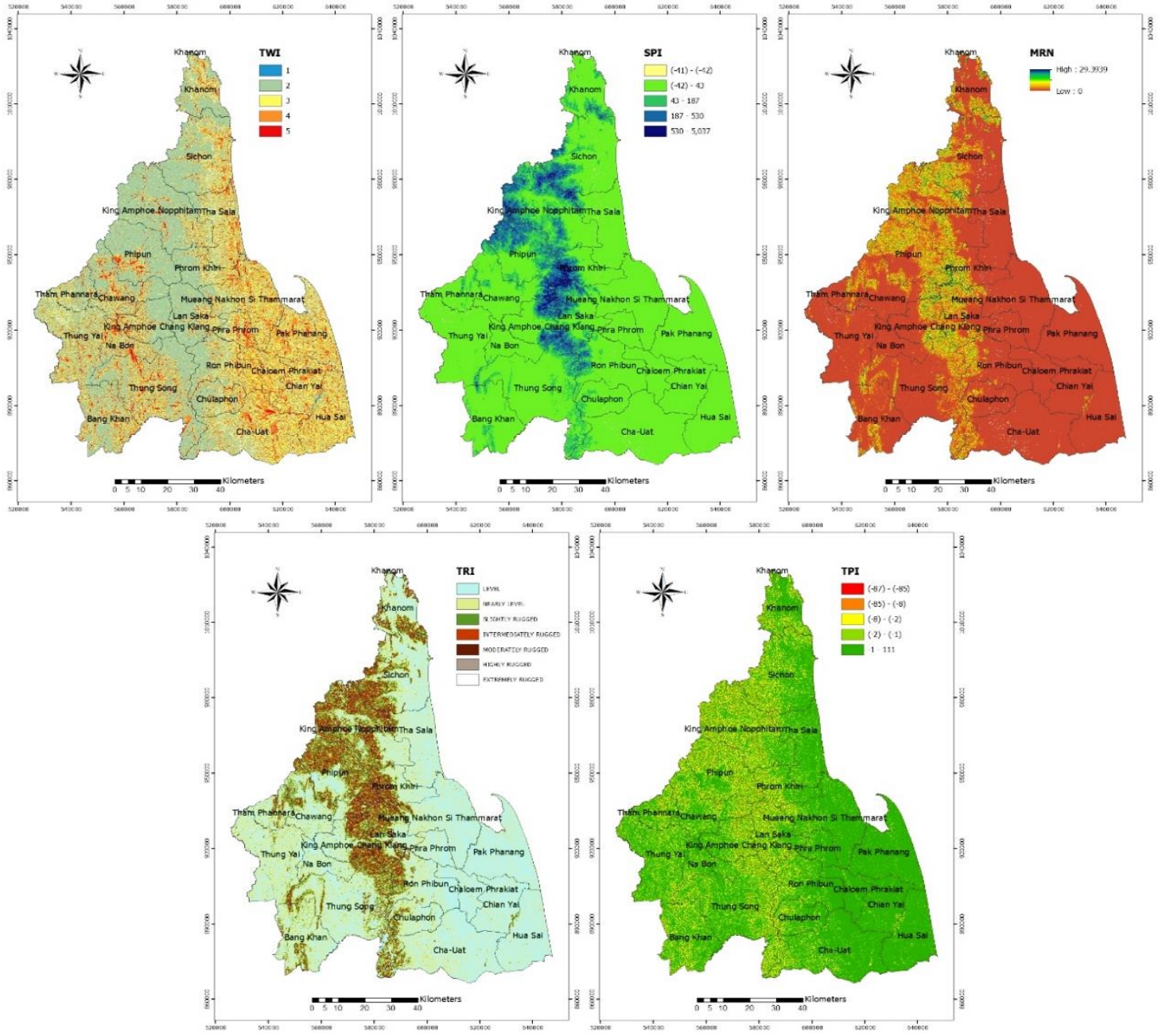

Figure 4. Map of NST showing the topographic index related to the debris flow susceptibility. (a) TWI, (b) SPI, (c) MRN, (d) TRI and (e) TPI index, respectively.

Table 2. Debris flow susceptibility of 10 parameters in this study.

Index	Class	Area (km^2)	Area (pixel)	Debris flow in class (pixel)	Fr
Slope	1	7461	48,383,561	20	0.89
	2	1088	7,056,736	5	1.54
	3	677	4,392,322	3	1.48
	4	341	2,210,878	1	0.98
	5	157	1,019,314	0	0.00
Aspect	flat	2,585	16,764,526	3	0.38
	N	1,107	7,181,414	6	1.81
	E	1,907	12,365,880	6	1.05
	S	1,785	11,575,550	8	1.50
	W	2,340	15,175,441	6	0.85
Solar Radiation	1	61	394,524	0	0.00
	2	353	2,289,517	0	0.00
	3	884	5,731,989	6	2.27
	4	8081	52,405,390	23	0.95
	5	346	2,241,391	0	0.00
Profile curvature	Concave	0	2,150	0	0.00
	Plan	9724	63,055,416	29	1.00
	Convex	1	5,242	0	0.00
Plan curvature	Concave	0	1261	0	0.00
	Plan	9724	63,059,630	29	1.00
	Convex	0	1,913	0	0.00
TWI	1	0	4	0	0.00
	2	5568	35,534,500	18	1.12
	3	1984	12,659,351	1	0.17
	4	1604	10,238,070	7	1.51
	5	0	3,634,635	2	1.21
SPI	1	0	1	0	0.00
	2	7747	50,236,985	25	1.08
	3	1206	7,818,722	3	0.83
	4	670	4,342,346	1	0.50
	5	103	664,757	0	0.00
MRN	1	7240	46,952,178	18	0.83
	2	1494	9,690,217	6	1.34
	3	597	3,873,767	3	2.68
	4	311	2,015,087	2	2.15
	5	82	531,562	0	0.00
TRI	1	4066	26,369,733	9	0.74
	2	3437	22,289,202	11	1.07
	3	1159	7,517,726	5	1.44
	4	711	4,610,115	4	1.88
	5	292	189,005	0	0.00
	6	53	346,078	0	0.00
	7	6	36,951	0	0.00
TPI	1	0	1	0	0.00
	2	218	1,410,864	0	0.00
	3	1324	8,583,802	0	0.00
	4	1043	6,760,724	0	0.00
	5	7141	46,307,420	0	0.00

3. Debris-Flow Susceptibility

3.1. Frequency Ratio (FR)

The FR model was used to calculate the weighting factors of debris flow susceptibility, with ten parameters: i) slope ii) aspect iii) solar radiation iv) TWI v) SPI, vi) TPI, vii) MRN, viii) TRI, ix) Plan curvature, x) and profile curvature.

The FR method has been widely used for debris flow susceptibility assessment (Li et al., 2017) based on the observed relationship between the scattering of debris and individual debris flow-related variables. This method demonstrates the relation between the location of the debris flow and the variables in the study area. The Fr can be calculated using the equation below (1).

$$F_r = \frac{N_i}{N} / \frac{S_i}{S} \qquad \text{Equation (1)}$$

Where **S** is the total number of pixels, **N** is the number of pixels in which the debris occurs, $\mathbf{S_i}$ is the number of pixels in this study variable, and $\mathbf{N_i}$ is the number of pixels in the **i** variable. A value greater than one indicates a stronger correlation. Meanwhile, values less than one indicate lower correlations on average (Lee et al., 2004a, 2004b). The Fr values for each factor were summed for each pixel. Consequently, the higher Fr, the higher the sensitivity. The smaller Fr, the more sensitive the debris flow is (Das and Raja, 2015). The computed Fr can be divided into five categories using the natural Jenks division: very low, low, medium, high, and high susceptibility (Das and Raja, 2015). The AUC (Area under the ROC Curve) method was used to assess the accuracy of FR results. It evaluates the accuracy of the model's predictions regardless of the classification threshold used. This study's AUC was 73.5%, and the R-squared (R^2) value was 0.9. (Figure 5). The R^2 is close to one, indicating that the regression model of debris flow susceptibility map is highly precise.

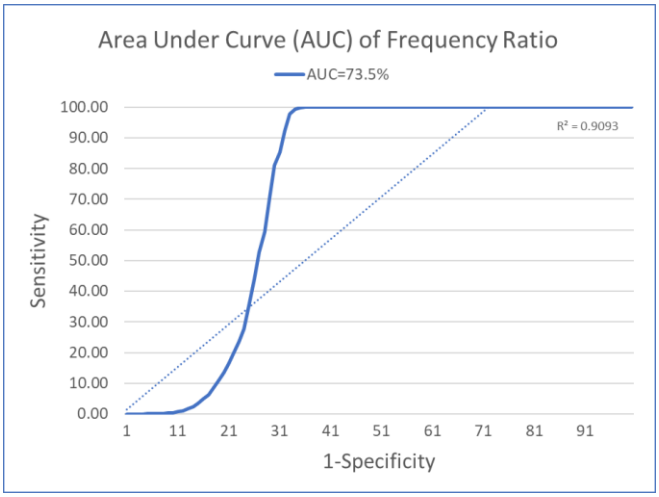

Figure 5. Showing area under curve (AUC) of frequency rai

3.2. Susceptibility Mapping

The result of debris flow susceptibility in NST is shown in Figure 6, with color classification based on the sensitivity level: i) dark green indicates a very low debris flow susceptibility area, ii) green indicates a low debris flow susceptibility area, iii) yellow indicates a medium debris flow susceptibility area, iv) orange indicates a high debris flow susceptibility area, and v) red indicates a very high debris flow susceptibility area. The level of debris flow susceptibility assessment can be divided into five groups, as show in Table 1: class 1 very low (0.85-6.38), class 2 low (6.38-7.91), class 3 medium (7.91-9.17), class 4 high (9.17-10.80) and class 5 very high (10.80-14.27). The area quantity can be sorted in descending order as follows: class 3 covers 4,501 km^2, class 4 covers 2,583 km^2, class 2 covers 1,534 km^2, class 5 covers 991 km^2 and class 1 covers the least area of 96 km^2 as shown in Table 3. According to the results of the analysis, a large portion of NST has been designated as a medium susceptibility area.

The other areas that were not mentioned above are considered to be very high susceptibility areas. Furthermore, these high susceptibility areas were discovered on the NST mountain range.

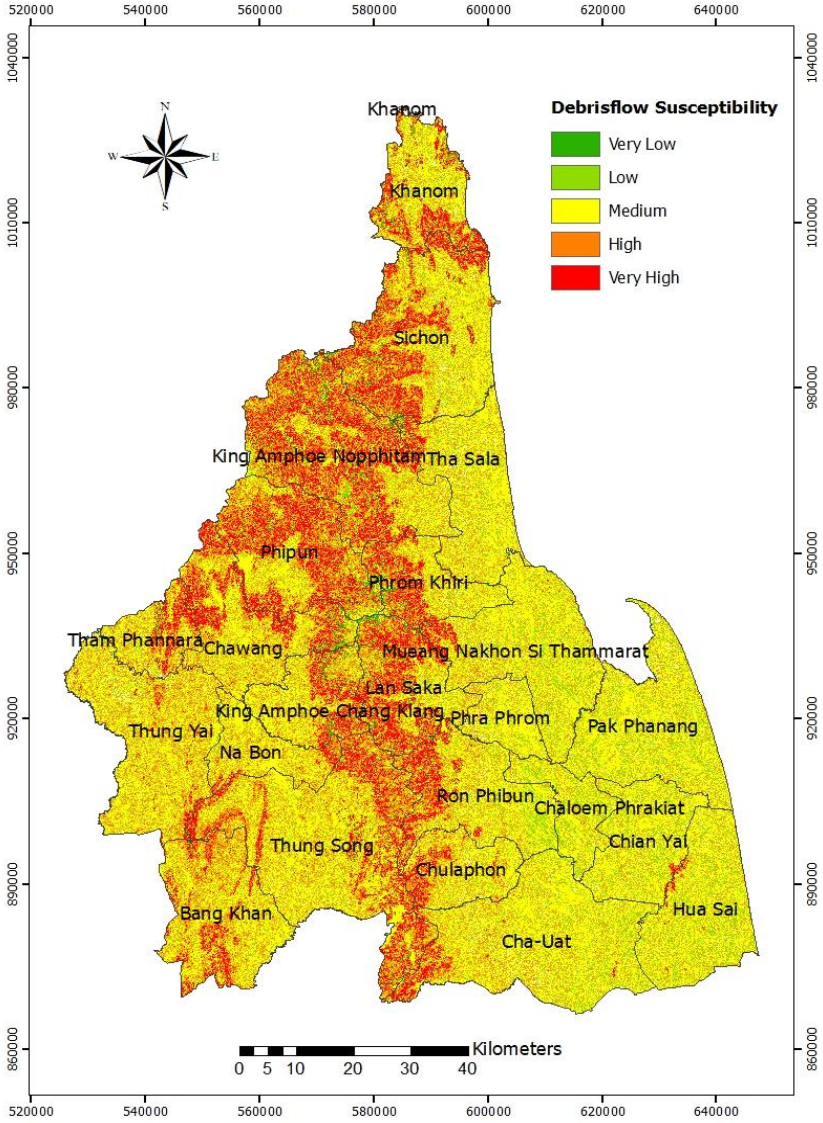

Figure 6. Map of NST showing debris flow susceptibility level obtained from this study. The color green means very low susceptibility, while the color red means very high susceptibility.

Table 3. Summary of the area in each debris flow susceptibility class in NST.

Class of debris flow susceptibility		Area (Km^2)
	Very low	96
	Low	1,534
	Medium	4,501
	High	2,583
	Very high	991

4. Discussion

According to the results (Figure 6), the debris flow susceptibility in the western and eastern NST, which are flat terrain, were classified as medium. It could be because these areas are furrowed, indicating the area's sensitivity. Because the method was analyzed using the terrain factor. There is no influence of debris flow on these zones.

Whereas the center of NST, which is a mountain range, presented high and very high classes. Thus, debris flow is less likely to occur in the west and east of NST. Meanwhile, areas with

steep slopes are more vulnerable to disasters than flat areas, which is one of the major causes of debris flow.

There may be experimental uncertainty due to calculations with different parameters. For example, some areas may have trash on the surface or may be landfill that was misdetected as debris. In that case, it may result in calculation errors.

However, the Fr approach is one of the most widely adopted methods to identify areas of susceptibility to debris flows with high precision. The study was performed using statistical parameters that were identified as the source of debris flow in NST. Furthermore, the parameters used in the previous studies were the same. The historical record of debris flow hazard matches the results obtained. It can be seen that debris flow occurred in the high-class susceptibility areas in the past.

5. Conclusion

Geomorphological indices are effective tools for assessing the influence of debris flow hazard assessment. In this study, the terrain analysis was assessed using DEM data with resolutions of 12.5 m. The FR method was used in this study to evaluate and weight factors that influence debris flow occurrences in ten parameters: slope, aspect, solar radiation, TWI, SPI, TPI, MRN, TRI, plan curvature, and profile curvature. These parameters are called debris flow susceptibility values, and can be classified into five categories based on the degree of sensitivity.

The high and very high classes (class 4 and class 5) of debris flow susceptibility have been found in a mountain range direction located in the center of NST. Meanwhile, the eastern and southern of NST have low and medium classes (class 2 to class 3).

Acknowledgement

This research was technically supported by T. Pichetsopon, T. Klomkliew, S. Chanprasit, and A. Puangjagta. We're sincerely grateful to the Department of Mineral Resource (DMR) for granting me permission to use essential data for this research. We appreciate the constructive feedback and suggestions by the editor and anonymous reviewers that enhanced the quality of this manuscript.

References

Angillieri, M. Y. E. (2020). Debris flow susceptibility mapping using frequency ratio and seed cells, in a portion of a mountain international route, Dry Central Andes of Argentina. CATENA, 189, 104504.

Chen, Y.R., Yeh, C.H., Yu, B., 2011. Integrated application of the analytic hierarchy process and the geographic information system for flood risk assessment and flood plain management in Taiwan. Nat. Hazards 59, 1261-1276.

Das, S., Raja, D.R., 2015. Susceptibility analysis of landslide in Chittagong City Corporation Area. Bangladesh. Int. J. Environ. 4, 157-181.

Department of Mineral Resources. [online]. March 30, 2012. Accessed from :http://www.dmr.go.th (Research date : 30 August 2020).

García-Rivero, A. E., Olivera, J., Salinas, E., Yuli, R. A., and Bulege, W. (2017). Use of hydrogeomorphic indexes in SAGA-GIS for the characterization of flooded areas in Madre de Dios, Peru. International Journal of Applied Engineering Research, 12(19), 9078-9086.

Lee, S., Choi, J., Min, K., 2004a. Probabilistic landslide hazard mapping using GIS and remote sensing data at Boun, Korea. Int. J. Remote Sens. 25, 2037-2052.

Lee, Saro, Choi, J., Woo, I., 2004b. The effect of spatial resolution on the accuracy of landslide susceptibility mapping: A case study in Boun. Korea. Geosci. J. 8, 51-60.

Li, L., Lan, H., Guo, C., Zhang, Y., Li, Q., Wu, Y., 2017. A modified frequency ratio method for landslide susceptibility assessment. Landslides 14, 727-741.

Marchi, L., Dalla Fontana, G., 2005. GIS morphometric indicators for the analysis of sediment dynamics in mountain basins. Environ. Geol. 48, 218-228.

Meinhardt, M., Fink, M., and Tünschel, H. 2015. Landslide susceptibility analysis in central Vietnam based on an incomplete landslide

inventory: Comparison of a new method to calculate weighting factors by means of bivariate statistics. Geomorphology 234: 80-97.

Pailoplee, S. (2019) 6 Disaster patterns of mass migration and the understanding of landslides. [online]. accessible from: http://www. mitrearth. org/7-3-mass-wasting/. (Research date: 18 September 2020)